Journal of Materials Chemistry B

PAPER

View Article Online
View Journal | View Issue

Cite this: J. Mater. Chem. B, 2015, 3, 9148

Fluorescent probes for the detection of cyanide ions in aqueous medium: cellular uptake and assay for β-glucosidase and hydroxynitrile lyase†

Hridesh Agarwalla,[a] Monalisa Gangopadhyay,[a] Dharmendar Kumar Sharma,[b] Santanu Kumar Basu,[c] Sameer Jadhav,[c] Arindam Chowdhury*[b] and Amitava Das*[a]

Received 7th September 2015,
Accepted 29th October 2015

DOI: 10.1039/c5tb01853f

www.rsc.org/MaterialsB

A chemodosimteric reagent (**1**) for the efficient detection of cyanide species (CN^- and/or HCN) in aq. medium as well as under physiological conditions has been described. Selective reaction of the cyanide species with this reagent in the presence of all common interfering anions, amino acids and glutathione (GSH) led to the generation of the corresponding cyanohydrin derivative. The formation of the cyanohydrin derivative of the probe is associated with a visually detectable change in solution fluorescence in aq. buffer medium with 1.9 μM NaCN, the threshold limit set by WHO for the safe drinking water and this makes this fluorogenic sensor an ideal candidate for in-field applications. An apparent switch on the luminescence response, ultralow detection limit, low response time, cell membrane permeability and insignificant toxicity are key features of a probe molecule, which gives it a distinct edge over previously reported chemodosimetric reagents for the detection of cyanide species (CN^- or HCN) in an aqueous environment. This methodology could be used for developing a generalized and efficient fluorescence-based assay for crucial enzymes like β-glucosidase and hydroxynitrile lyase. Furthermore, spectrally-resolved fluorescence microscopy measurements on single-cells revealed that this sensor molecule could also be used for imaging the cellular uptake of cyanide species from aq. solution contaminated with NaCN. Our results confirmed that statistical analysis of integrated intensity and transition energy obtained from the emission spectra collected over various microscopic sub-cellular regions can potentially be used to discriminate the effects of local cellular environments and that due to cyanide detection.

Introduction

The design and synthesis of new chemosensors for the recognition of specific anions that have serious biological effects is of immense importance for chemists and biologists who are active in the area of diagnostics as well as in studies involving biological and environmental events.[1] Among various toxic anions, the cyanide ion (CN^-) is considered to be the most toxic and its acute toxicity towards mammals primarily arises from its adverse influences on the central nervous system.[2] Cyanide primarily binds to metallic cofactors in metalloenzymes, adversely influencing the enzyme and cell function. It inhibits the activity of Cytochrome-*c* oxidase and causes histotoxic hypoxia, which further adds to the toxicity by reducing the unloading gradient of oxyhemoglobin.[3] Cyanide is also known to inhibit the activity of enzymes like catalase, peroxidase, hydroxocobalamin, phosphatase, tyrosinase, ascorbic acid oxidase, xanthine oxidase, and succinic dehydrogenase. These also contribute to cyanide's acute toxicity.[4,5,9] Despite influences on living organisms, cyanide is extensively used in various industries like metal gold mining, electroplating, petrochemical, synthetic fibers and the resin industry.[6] Regardless of environmental consciousness, a certain amount of this toxic ion escapes into the environment either as water soluble cyanide species or as HCN. Some fruits and vegetables such as cassava, lima beans, and bitter almond also contain high levels of cyanogenic glycosides which are potential sources of cyanide in the presence of certain enzymes and can be lethal if not processed properly before consumption.[7] The World Health Organization (WHO) has set the maximum allowed cyanide contaminant in drinking water to be 1.9 μM.[8] Due to its extreme physiological toxicities, a suitable reagent for the efficient and preferential recognition of cyanide species in

[a] Organic Chemistry Division, CSIR-National Chemical Laboratory, Pune 411008, India. E-mail: a.das@ncl.res.in; Fax: +91(0)25902629; Tel: +91(0)25902385
[b] Department of Chemistry, Indian Institute of Technology Bombay, Powai, Mumbai 400 076, India
[c] Chemical Engineering, Indian Institute of Technology Bombay, Powai, Mumbai 400 076, India. E-mail: arindam@chem.iitb.ac.in; Fax: +91(0)22-2576 7152; Tel: +91(0)22-2576 7154

† Electronic supplementary information (ESI) available. See DOI: 10.1039/c5tb01853f

water, more specifically under physiological conditions, is a fundamental requirement.[9] If such a reagent allows the recognition process through a fluorimetric response, the option of using such a probe molecule as an imaging reagent for the detection of cellular uptake of cyanide species becomes a possibility.[10]

The most common approach for the recognition of CN^- is based on hydrogen bonding (H-bonding) interactions, which often encounter interference from F^-, OAc^- and HPO_4^{2-}/PO_4^{3-}.[11] In general, such a methodology is suitable for studies performed in non-aqueous medium and fails in aqueous medium due to the high hydration energy of CN^- (-339 kJ mol^{-1}). To get around this problem, researchers have adopted either M^{n+}–CN^- (M^{n+} is metal ions) coordination or the chemodosimetric process, which involves enthalpy change that surpasses the otherwise high solvation enthalpy of CN^- in water.[12] In the chemodosimetric process, the nucleophilicity of cyanide has been utilized for designing such reagents.[13–16] The reduced nucleophilicity of CN^- due to its efficient solvation in aq. medium generally retards its reactivity in aq. medium. Relatively long reaction time and limited solubility of such reagents in pure aqueous medium are the major bottlenecks for the use of such reagents for any practical application. These limitations leave a distinct scope for the development of an efficient molecular probe for the detection of CN^- and/or HCN in an aqueous environment.

To address these limitations researchers have put effort in designing new molecular probes that could show a fluorescence response upon reaction with CN^- and/or HCN under physiological conditions. The impact of such reagents will be greater if they could be used as imaging reagents for the detection of cellular uptake of cyanide species. Such reagents could also be used to develop appropriate enzyme assay protocols for synthesizing important industrial enzymes.[17,18] Though there are few reports on fluorescence on- based reagents for the effective recognition of CN^- and/or HCN in an aqueous environment and their use as imaging reagents,[10] there are only two literature reports on using such reagents for developing an enzymatic assay.[17] β-Glucosidase is an important enzyme that plays an important role in a variety of fundamental biological processes like liberation of aromatic compounds from glucosidic precursors or detoxification of cyanogenic glycosides.[19] β-Glucosidase, obtained from bitter almond, is known to have three different enzymes namely, amygdalin lyase, prunasin lyase and hydroxynitrile lyase (HNL),[20] each one is specific for one hydrolytic stage (*vide infra*). Thus, it is expected to release CN^- and/or HCN upon reacting with amygdalin ([*O*-β-D-gluco-pyranosyl-(1-6)-β-D-glucopyranosyloxy]benzeneacetonitrile), an important cyanogenic glycoside found in various fruits and seeds.[21] Hydroxynitrile lyases are a versatile group of enzymes, which play a significant defensive role in plant systems against microbial attack and also cause the release of HCN or CN^- from biologically active cyanohydrin like mandelonitrile.[20]

In this article, we report a benzooxazine derivative **1** (Scheme 1) as a chemodosimetric reagent for the effective detection of CN^- or HCN in aqueous medium under physiological conditions without any interference from other competing anions, amino acids and biothiols (*e.g.* cysteine, homocysteine and glutathione). This reaction was found to be associated with a detectable change in solution colour and fluorescence, upon formation of the corresponding cyanohydrin derivative. A significant enhancement in the blue-shifted luminescence intensity helped us in the quantitative estimation of cyanide species under physiological conditions and in using it as an imaging reagent for the detection of cellular uptake of CN^-. Short reaction time ($\leq$10 min at RT), a detection limit (0.286 μM) that is lower than the permitted level (1.9 μM) of cyanide in safe drinking as per WHO norms, with a visually detectable change in solution fluorescence for the naked eye detection of solution having 1.9 μM of CN^- under physiological conditions, cell membrane permeability and insignificant toxicity towards live cells give this probe molecule a distinct edge over most other molecular sensors reported to date for cyanide ions. Furthermore, we have also reported the results of our studies for developing a generalized assay for β-glucosidase and HNL based on a luminescence on response. To the best of our knowledge there are only two previous reports on the use of such molecular probes for developing enzymatic assay.[17] The feasibility of using this reagent for the imaging of cyanide uptake in cellular media was investigated by spectrally-resolved fluorescence microscopy measurements. Although conventional intensity based imaging may be inadequate due to non-uniform intracellular partitioning of sensors, which can result in a considerable spatial variation of intensities,[22] we have shown that it is essential to construct distributions of the two spectral parameters, namely integrated intensities and transition energies, using a large number of emission spectra acquired from various microscopic sub-cellular regions in order to confirm HCN and/or CN^- detection.

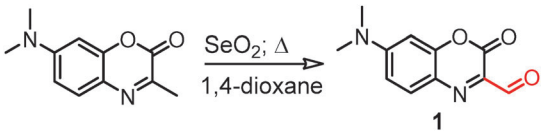

Scheme 1 Schematic representation of the synthesis of **1**.

Experimental section

All the basic chemicals, reagents and solvents used for this study were of analytical grade and were purchased from commercial suppliers and were used without prior purification, unless mentioned otherwise relevant details are provided in the ESI.† Details about the sample preparation, cell culture and instrumentation are also provided in the ESI.†

Results and discussion

Reagent **1** was prepared following a previously reported procedure,[23] with necessary modification (Scheme 1). Oxidation of the methyl group with SeO_2 yielded the desired product **1**. After initial purification of the reagent (**1**) by column chromatography, using ethyl acetate-petether (1 : 4, v/v) as an eluent and

silica gel (100–200 mesh size) as the stationary phase, reagent **1** was further purified by recrystallization from *n*-hexane to ensure the desired purity. Appropriate characterization and purity of the isolated compound were ascertained based on the results of various analytical and spectroscopic (^{1}H & ^{13}C NMR and ESI-Ms) studies. These are provided in the ESI.†

For the present study, typically solutions having an effective concentration of 1.2 mM for CTAB and 10 mM for aq. HEPES buffer with an effective solution pH of 7.2 were used. To 5 ml of this solution, 20 μL of the stock solution of **1** (5.0×10^{-3} M in DMSO) was added and this solution was used for all the spectroscopic studies, unless mentioned otherwise. The use of such a micellar structure as ''solubilizer'' for organic molecules in water is not uncommon in the literature and we have adopted this ideology for our studies under physiological conditions.[24] The mean diameter of the CTAB micelles at the above mentioned aq. buffer medium was 6.3 nm, while that having reagent **1** trapped inside the hydrophobic cavity was 4.1 nm (ESI,† Fig. S21). The absorption spectrum of **1** (20 μM) in an essentially aqueous HEPES buffer medium (aq. buffer : DMSO of 250 : 1, v/v; pH 7.2) having 1.2 mM CTAB showed a high energy band at 300 nm ($\varepsilon = 7.46 \times 10^3$ M^{-1} cm^{-1}) and a low energy band at 505 nm ($\varepsilon = 2.26 \times 10^4$ M^{-1} cm^{-1}). The band at 300 nm was attributed to a π–π* transition, whereas the band at 505 nm was assigned to be an intra-molecular charge transfer (CT) process involving dimethylamine as the donor and the carbonyl group as an acceptor moiety. This solution shows a weak emission (Φ = 0.009) when excited at 430 nm (Fig. 1b). The electronic spectra of reagent **1** in identical solvent medium were recorded in the absence and presence of all common amino acids (*e.g.* AAs: Ala, Ser, Trp, Met, Val, Arg, Phe, Pro, Thr, Gly, Lys, His, Asp, Ile, Leu, Glu, Tyr, Cys, and Hcy), glutathione (GSH) and common anionic analytes (*e.g.* F^-, Cl^-, Br^-, I^-, CN^-, CH_3COO^-, $H_2PO_4^-$, $P_4O_7^{4-}$, SO_4^{2-}, NO_2^-, NO_3^- and HSO_3^-) (Fig. 1a). A distinct blue shift of 80 nm of the CT band at 505 nm was observed in the presence of added CN^- (Fig. 1a inset) and HSO_3^- (ESI,† Fig. S22) with an associated visually detectable change in solution colour from red to yellow.

Reaction of the aldehyde functionality of **1** with cyanide species (CN^- and/or HCN) was expected to yield the corresponding cyanohydrin derivative and this adversely influenced the CT transition dipole, which was accounted for the observed blue shift. All other anions, biothiols and amino acids failed to induce such reaction and these results clearly revealed the specificity of probe **1** towards CN^- and/or HCN in aq-buffer medium (pH = 7.2). An earlier report revealed that this reagent can be utilized for the chemodosimetric detection of Cys and Hcy in acetonitrile-aq. HEPES buffer (10 mM, pH = 7.2) solution (3 : 7, v/v; RT) and no other amino acid was found to interfere in the detection process.[23] However, our studies revealed that the solution luminescence of **1**, trapped inside the micellar structure of the CTAB in an essentially aq. HEPES buffer medium (aq. buffer : DMSO of 250 : 1, v/v), remained practically invariant in the presence of externally added 10 mole equivalents of various amino acids (AA: Ala, Ser, Trp, Met, Gln, Val, Arg, Phe, Pro, Thr, Gly, Lys, His, Asp, Ile, Asn, Leu, Glu, Tyr, Cys, Hcy, and GSH) and

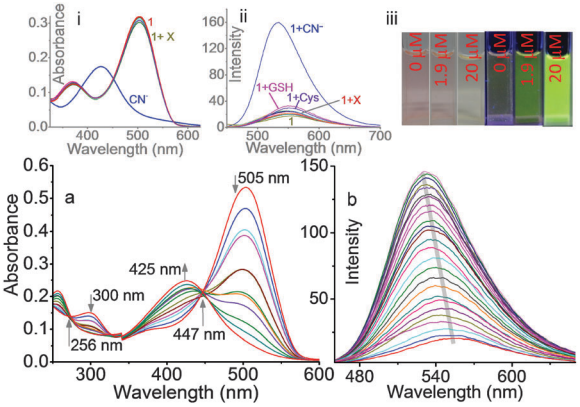

Fig. 1 Changes in (a) absorption and (b) emission spectra of **1** (20 μM) in the presence of 0–3 mole equivalents of NaCN: inset: (i) change in the absorption and (ii) emission spectra of **1** (20 μM) in the absence and presence of 10 equivalents of X (X = F^-, Cl^-, Br^-, I^-, CN^-, HSO_4^-, NO_2^-, NO_3^-, OAc^-, and $H_2PO_4^-$), different AAs and 10 mole equivalents of GSH. λ_{Ext} of 430 nm was used for all luminescence studies; inset (iii): photograph showing the visually detectable changes in solution colour and fluorescence for **1** (10 μM) in the presence of 1.9 μM (threshold concentration of CN^- for safe drinking water) and 20 μM of NaCN. All studies were performed in 10 mM aq. HEPES-DMSO (250 : 1, v/v) having 1.2 mM CTAB (pH 7.2) and a handheld 365 nm UV lamp was used for illumination.

all common anions (*e.g.* F^-, Cl^-, Br^-, I^-, CH_3COO^-, $H_2PO_4^-$, HSO_3^-, $P_4O_7^{4-}$, HSO_4^-, NO_2^- and NO_3^-) except HSO_3^- and CN^- (Fig. 1b inset). A switch on the luminescence response was observed for CN^- with a blue shift of ~15 nm for the band maximum, while a very little enhancement in emission intensity with emission maxima at 548 nm was observed for Cys or GSH. Hcy failed to induce any change in the spectral pattern for probe **1** (Fig. 1b). Presumably, the micellar structure of CTAB not only helped in solubilizing probe **1** in aq. buffer medium, but the nano-compartments also provided a favorable hydrophobic environment for the interaction of probe **1** and CN^-. The use of such micellar structures in the design of suitable sensors for cationic and anionic analytes has been reported recently.[24] Interestingly, DLS studies with the solution after the completion of reaction of reagent **1** with CN^-/HCN revealed a small increase in the micellar diameter (5.3 nm) (ESI,† Fig. S21), suggesting that the micellar structure remained intact even after the reaction of **1** with HCN/CN^-, though with a little broader diameter distribution. Analogous changes were also observed for HSO_3^-, although the extent of changes was little less as compared to that observed for CN^-.

Systematic absorption spectral titrations were carried out for varying [CN^-] (0–60 μM), while effective [**1**] was maintained at 20 μM. Upon gradual increase of [CN^-], the CT band with maxima at 505 nm was found to bleach with a concomitant increase of a new band with maximum at 425 nm (Fig. 1a). No further change in the absorption spectral pattern was observed after 3 mole equivalents of [CN^-]. The titration spectral pattern also revealed three simultaneous isosbestic points at 272 nm, 340 nm and 447 nm, which indicated that the reactant and the product (absorbing species) existed in equilibrium.

As mentioned earlier, steady state emission studies showed a weak emission band with λ_{Ems}^{Max} of 548 nm (Φ = 0.009; λ_{Ext} of 430 nm)

for **1** (Fig. 1b). Systematic emission titration with 20 μM of **1** revealed an appreciable enhancement in emission intensity (Φ = 0.05, λ_{Ext} = 430 nm) with a slight blue shift in the band maximum (λ_{Ems}^{Max} = 535 nm) upon gradual increase in [CN^-] (0–3 mole equivalent) (Fig. 1b). Relative luminescence quantum yield for **1** and **1**.CN^- were evaluated using coumarin-6 (Φ = 0.78) in ethanol solution as a standard. The excitation spectra of **1** in the presence of 3 mole equivalents of CN^- (λ_{Ems} = 535 nm) showed a maxima at ~425 nm and this implied that the final emission state for the cyanohydrin derivative was different from that of reagent **1** (ESI,† Fig. S5). Results of interference studies carried out in the presence of 200 μM of all common anions and amino acids/biothiols (ESI,† Fig. S6) using 20 μM **1** in 10 mM aq. HEPES buffer and 1.2 mM CTAB (pH = 7.2) clearly revealed that there was no interference from other anions and AAs, while interferences from GSH and Cys were kept to a bare minimum under the present experimental conditions. As discussed earlier, interference was observed only from hydrogen sulphite. Analogous interference experiments were also performed with GSH or Cys in the presence of 50 mole equivalents of NEM (*N*-ethylmaleimide), added prior to the addition of reagent **1**. The very small decrease in emission intensities that were earlier observed at 535 nm was restored (ESI,† Fig. S7). NEM is known to selectively block GSH or Cys and this confirmed that the interference from GSH and Cys in the quantitative estimation of CN^- was truly minimal. Thus, these results clearly illustrate the specificity of the present reagent towards CN^- under the present experimental conditions. Job plot analysis confirmed a 1 : 1 binding stoichiometry (ESI,† Fig. S8) and the increase in emission intensity as a function of [CN^-] was found to be linear for [CN^-] of the 0–8 μM region ([**1**] is 10 μM). This linear calibration plot could be used for the quantitative estimation of CN^- and/or HCN in aq. buffer medium (ESI,† Fig. S9). The lowest detection limit of CN^- was evaluated to be 2.86×10^{-7} M, which is much lower than the threshold limit set by WHO (1.9 μM) for safe drinking water.[8a] A visually detectable change in solution fluorescence was also observed for solution having a [NaCN] of 1.9 μM (Fig. 1, inset iii) and this has made this reagent suitable for a "*yes–no*" type binary response for the in-field detection of CN^- and/or HCN in pure aqueous medium (ESI,† Fig. S10). Examples of such fluorescence-based reagents are rather rare in the existing literature.[8b,c] The results of our studies revealed that the efficiency of the detection process for HSO_3^- was lower as compared to that for cyanide (ESI,† Fig. S22 and S23).

The spectral response of probe **1** (20 μM) in an essentially aq. HEPES medium having 1.2 mM CTAB solution was examined in the absence and presence of 10 mole equiv. of NaCN at different pH values (pH = 3–9). The results revealed that the absorbance at 425 nm as well as the steady state emission intensity at 535 nm for solution **1** remained practically invariant over the entire pH range that we studied. However, the reaction of **1** with the cyanide species was found to be efficient over the pH range of 5–8 (ESI,† Fig. S11 and S12). Time dependent fluorescence at 535 nm was monitored with different concentrations of CN^-, which revealed that the reaction was completed within 10 minutes (ESI,† Fig. S13). Thus, results of all spectroscopic studies confirmed that probe **1** could preferentially react with cyanide species in an essentially aq. buffer medium within the pH range of 5–8, while the presence of the large excess of GSH, AAs and various anionic analytes failed to interfere with the detection processes. Furthermore, changes in electronic and luminescence spectral patterns in the visible region were large enough for CN^- to induce a visually detectable change in the solution colour to allow its naked eye detection (ESI,† Fig. S10).

To ascertain the formation of a corresponding cyanohydrin derivative, ^{1}H NMR spectra were recorded (in DMSO-d_6) in the absence and presence of different concentrations of CN^- (TBACN). Upon formation of cyanohydrin, the sharp signal for H_{CHO} at 9.83 ppm disappeared with a simultaneous appearance of a new signal at δ = 8.33 ppm (ESI,† Fig. S14). This new signal was ascribed to the $H_{-CH(OH)(CN)}$ proton of the newly formed cyanohydrin derivative. Furthermore, anticipated upfield shifts were also observed for other aromatic protons of reagent **1**.[13c,14b] The formation of the corresponding cyanohydrin was also confirmed by the signal at *m*/*z* = 245.0784 (*m*/*z* calcd. is 245.08 for **1** + CN^- + H^+) (ESI,† Fig. S15).

Having a molecular probe that could effectively detect CN^- and/or HCN under physiological conditions, we explored the possibility of developing a fluorescence-based assay for studying the hydrolysis of amygdalin by an important enzyme like β-glucosidase. β-Glucosidase plays diverse and important roles in prokaryotes and eukaryotes.[25–27] This class of enzymes present in bacteria and fungi are crucial for biomass conversion,[25] while for animals these are essential for glycosphingolipid metabolism.[26] In higher plants, these are used in chemical defence against herbivores and pathogens through cyanogenesis in plants, lignifications and regulation of phytohormones by inducing hydrolysis of their inactive hormone–glucoside conjugates.[27] Considering the significance of the enzymatic activity of β-glucosidase, developing an effective and sensitive assay for this crucial enzyme is of vital importance. Enzyme assays are important to assess the performance of enzyme in high-throughput screening. Conventionally, chromatographic methodology or oligosaccharide substrates functionalized with an appropriate fluorophore moiety through an ether linkage is used for developing an assay for such enzyme.[28] However, the synthesis of such functionalized oligosaccharide substrates generally involves intricate synthetic methodologies and above all, the solubility of such a reagent in aqueous medium or under physiological conditions is limited. This means the use of such fluorogenic oligosaccharides is in slurry, which is barely homogeneous.[28] Considering these limitations, the possibility of using a small molecule that shows a fluorescence turn-on response upon quantitative reaction with the hydrolyzed product of the β-glucosidase has significance for developing a more efficient assay methodology. To explore such a possibility for **1**, this reagent was used to assay β-glucosidase activity on amygdalin, a well known cyanogenic glycoside found in bitter almond. Amygdalin is known to release CN^- and/or HCN depending on media pH upon metabolism by β-glucosidase (ESI,† Scheme S1).[29] The results discussed above clearly indicate that CN^- and/or HCN

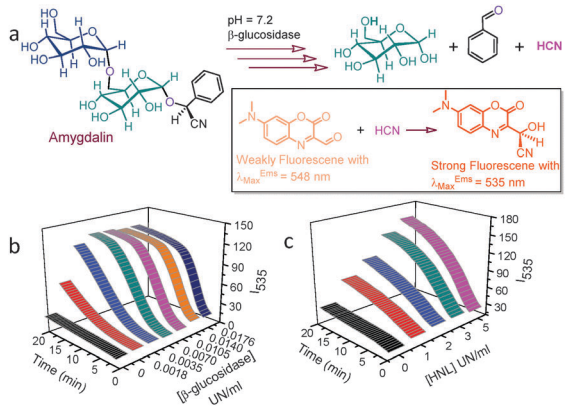

Fig. 2 (a) Schematic representation of hydrolysis of amygdalin by β-glucosidase. Time dependent luminescence intensity measurements (λ_{Ems} = 535 nm & λ_{Ext} = 430 nm) of **1** (20 μM) in the presence of (b) amygdalin (1 mM) with varying concentrations of β-glucosidase (0–0.0176 UN ml^{-1}) at pH 7.2 and (c) mandelonitrile (1 mM) with varying concentrations of HNL (0–5 UN ml^{-1}) at pH 6.5. All studies were performed in an essentially aq. buffer (10 mM aq. HEPES-DMSO (250 : 1, v/v)) medium having 1.2 mM CTAB.

could react with probe **1** to yield a corresponding cyanohydrin derivative with significant enhancement in luminescence with maxima at 535 nm (Fig. 2a). Accordingly, the hydrolysis reaction of amygdalin by β-glucosidase in aqueous medium pH of 7.2 was monitored through the increase in luminescence intensity of **1** (20 μM) at 535 nm as a function of time as well as a function of the [β-glucosidase] (0–0.0176 UN ml^{-1}) in 10 mM HEPES/1.2 mM CTAB pH 7.2, with amygdalin (1 mM) (Fig. 2b). In the absence of β-glucosidase, fluorescence intensity at 535 nm remained unaltered; while a subsequent increase in emission intensity was observed as a function of [β-glucosidase]. At pH 7.2, cyanide (pK_a = 9.21) is expected to exist in solution predominantly as HCN (~99%). Thus, HCN produced through hydrolysis of amygdalin reacted with the probe molecule (**1**) to generate the corresponding cyanohydrin compound with an associated increase in emission intensity at 535 nm. For [β-glucosidase] of 0.0176 UN ml^{-1}, reaction was mostly complete (~90%) within 5 min. To confirm that the emission enhancement was solely due to the reaction of HCN and/or CN^- that was produced through hydrolysis of amygdalin by β-glucosidase, control experiments in the absence of amygdalin under otherwise identical experimental conditions were carried out and no enhancement in emission intensity was observed. This confirms that emission enhancement occurs only when both amygdalin and β-glucosidase are present and HCN/CN^- is produced by the hydrolysis of amygdalin by β-glucosidase (ESI,† Fig. S16). We have also performed control experiments under identical experimental conditions with other disaccharides that did not contain any cyano group, but are known to be hydrolysed by β-glucosidase to produce glucose and benzaldehyde. Accordingly, analogous studies with two different disaccharides (maltose and lactose) and glucose did not show any change in luminescence intensity at 535 nm, compared to changes that were observed for amygdalin (ESI,† Fig. S16).[30] These results further confirm that other byproducts of the hydrolysis reaction, *i.e.*, glucose and benzaldehyde, do not have any influence in the emission enhancement. Thus, the above discussed methodology could be utilized for the development of an effective assay for a significant enzyme like β-glucosidase for studying the hydrolysis of amygdalin.

Another set of control experiments with [β-glucosidase] (0.0105 UN ml^{-1}) in 10 mM HEPES/1.2 mM CTAB pH 7.2, and amygdalin (1 mM) were performed in the absence and presence of HNL (3 UN ml^{-1}) and luminescence intensity of the respective solution was monitored for 10 minutes. Similar emission intensities at 535 nm for both solutions ensured complete degradation of amygdalin by β-glucosidase into two equivalents of glucose, and one equivalent of benzaldehyde and cyanide species (ESI,† Fig. S17). Michaelis constant (K_m) was evaluated from the time dependent luminescence studies of **1** (20 μM) and β-glucosidase (0.014 UN ml^{-1}) with varying [amygdalin] (0.4–1.0 mM) in solution. Initial rates (v) were calculated for the first five minutes and K_m (4.68 × 10^{-4} M) was evaluated from the slope of the plot of 1/v *vs.* 1/[amygdalin] (ESI,† Fig. S18). Slight variation in the evaluated K_m value, from those reported in the literature,[17b,19a] could be ascribed to slightly different assay conditions. Thus, our studies confirmed that reagent (**1**) can be utilized as a fluorescence based assay for the industrially and biologically significant enzyme β-glucosidase and such examples are scarce in the contemporary literature. To illustrate the versatility of probe molecule **1**, as a reagent for developing luminescence based enzymatic assay, a similar enzymatic process, the hydrolysis of mandelonitrile (MNDL) by HNL (from *Arabidopsis thaliana*) into the corresponding benzaldehyde and cyanide species, was also examined (Fig. 2c). Luminescence enhancement was observed upon hydrolysis of MNDL with HNL and this could be utilized for evaluating the Michaelis constant (5.76 × 10^{-4}) for HNL, (ESI,† Fig. S19), which was close to the value reported earlier for this reaction.[17a]

Finally, we have explored the possibility of detection and imaging of the cellular uptake of cyanide ions in cellular environments using the apparent switch on the fluorescence response of this reagent. For this purpose, human breast adenocarcinoma cells (MDA-MB-231 cells) were treated with **1** (10 μM) at 37 °C. These cells were then washed twice with phosphate buffer saline solution (PBS) to remove excess adhered probe molecules. MDA-MB-231 cells, pre-treated with **1**, were incubated with an aq. solution of CN^- (200 μM) for 15 minutes and washed with PBS, following which both phase contrast and fluorescence intensity images were collected in the absence and presence of CN^- (Fig. 3). Fig. 3B and C clearly demonstrate that probe molecule **1** is cell permeable, while MTT assay shows the nominal toxicity of the sensor molecule (ESI,† Fig. S20).

These results suggest that probe **1** could be utilized for the detection of uptake of cyanide species in cells pre-exposed to an aq. solution of NaCN. Fluorescence intensity and overlay images (Fig. 3B, C, E and F) illustrate that cells treated with only **1** have very weak emission whereas those incubated with CN^-, showed a considerable enhancement in the fluorescence intensity (Fig. 3E and F). We note, however, that these intensity images (Fig. 3B and E) provide an average behaviour of the

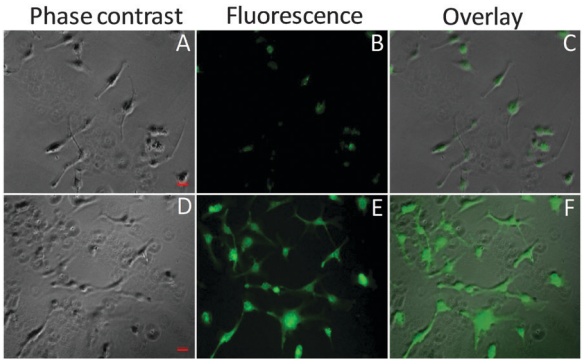

Fig. 3 Phase contrast (left panels), fluorescence microscopy (middle panels) at 10× magnification, and the overlay images (right panels) of the same lateral area for MDA-MB-231 cells incubated with **1** (10 μM), in the absence (A–C) and presence (D–F) of NaCN (200 μM). Scale bar is 50 μm.

intensity response of probe **1** in an ensemble of cells, and it is inappropriate to comment on the spatial distribution of cyanide uptake from intensity measurements alone.

The resulting spatial variation in emission intensity of probe **1** due to non-uniform labelling of cells can be easily noticed in the higher magnification TIRF images (Fig. 4a and b). Furthermore, a close inspection of individual cells revealed the existence of locally emissive bright spots over a relatively weak cytoplasmic background, suggesting the accumulation of probe **1** in various microscopic sub-cellular domains within the cytoplasm of each cell even in the absence of cyanide (Fig. 4a). As a result, it was challenging to determine whether the enhancement of intensity within the sub-cellular regions arises from sensor accumulation in different microscopic spatial locations or due to the formation of strongly luminescent cyanohydrin derivatives upon reaction with cyanide species. Therefore, using only emission intensity as a sole observable, it was not possible to determine the efficiency of probe **1** for cyanide detection in different sub-cellular regions. Since probe **1** also undergoes a blue shift in its emission spectral envelope upon cyanide binding, we surmised that colorimetric discrimination between various regions in individual cells might provide more insight into cyanide detection in cells. However, solution studies point out that the spectral blue-shift was not pronounced (~15 nm) and therefore it was extremely challenging to detect the subtle color changes either visually or by dual-color imaging using energetically separated emission filters.

This prompted us to perform spatially-resolved fluorescence spectroscopy measurements on single cells labelled with probe **1**. Fig. 4c and d showed several characteristic emission spectra of probe **1** that were collected from different microscopic domains (0.5 × 0.5 μm^2) of a single cell, in the absence and presence of cyanide ions. It should be noted that these representative emission spectra shown in Fig. 4c and d are only a few of several hundreds of emission profiles collected from various local intracellular regions, over 15 different cells. Spatially-resolved spectroscopy revealed that the emission maxima of probe **1** in the absence of cyanide were located close to ~550 nm, which shifted to slightly shorter wavelengths along with enhanced emission intensities (for a considerable fraction of spatial locations) in the presence of cyanide. We note, however, that due to the non-homogeneous cellular medium, probe **1** exhibited a range of emission maxima, likely arising from fluctuations in local environmental polarity where the probes were embedded. To understand whether an observed spectral shift was indeed due to the detection of cyanide in a particular microscopic (sub-cellular) region, we extracted the integrated intensity and transition energy from each emission profile, and generated a scatter plot considering a large number (~470) of such spatially-resolved emission spectra in the absence and presence of cyanide (Fig. 4e and f, ESI,† Fig. S24). In this scatter plot, we found several spots which have similar values of both intensity and transition energies in the absence and presence of cyanide. However, the qualitative change in the shape of the scatter plots indicated that a large fraction of spectra have relatively high values of intensity as well as transition energy, a signature of cyanide detection. Therefore, those spatial locations where there was a significant (>5 nm) blue-shift of spectral peak

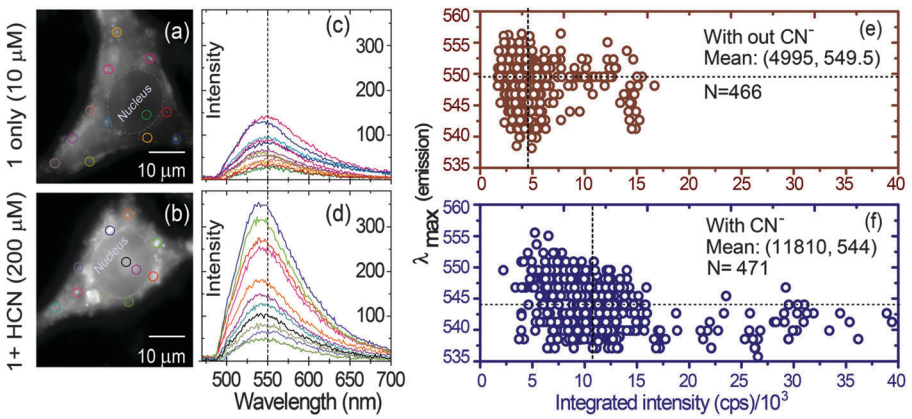

Fig. 4 TIRF microscopy images (a and b) of single MDA-MB-231 cells treated with **1**, and representative spatially-resolved emission spectra (c and d) in the absence (a and c) and presence (b and d) of cyanide. Circles within the images represent microscopic regions (~0.5 × 0.5 μm^2) within different locations of the cell from which fluorescence spectra were acquired (color matched with circles). Scatter plots (e and f) of emission spectral maxima against integrated intensity (circles) in the absence (e) and presence (f) of cyanide species depicting the variation in sensing efficiency in cellular environments.

positions along with considerable intensity enhancement of probe **1** were likely to have more cyanide present as compared to other locations (with nominal shift) within the cellular environment. The observed heterogeneity in the emission spectra collected from different microscopic regions also indicates that, for a given (fixed) incubation concentration of cyanide ions, the proportion of cyanide-bound probe **1** present in different sub-cellular regions is likely to be non-uniform.

To illustrate the relative changes in the spectral response in various microscopic sub-cellular regions, we have constructed distributions of both spectral peak positions (transition energies) and emission intensity, which are overlaid on the scatter plots (Fig. 4e, f and Fig. S24, ESI†). We find that the mean value (standard deviation) of transition energy shifts from ~549 nm (3.5 nm) to ~544 nm (4 nm) in the presence of cyanide, while the average emission intensity increases from 4995 cps to 11 810 cps. The widths of distributions in the absence of cyanide can be used as a qualitative indicator for a sensory response due to local environmental fluctuations within cells. Therefore, the relatively large change in both these distributions in the presence of cyanide suggests that the sensor's spectral response due to cyanide detection is greater than those arising from changes in the local environment. Attempts are currently being made to develop a methodology to further discriminate between spectral variations arising from local environmental fluctuations in the vicinity of probe **1** and the effect of cyanide binding/detection at different sub-cellular regions.

Conclusions

In summary, we have demonstrated that a simple luminophore could be used as a chemodosimetric probe for the specific recognition of cyanide species (CN^- and/or HCN) in an ensemble of all common anions, amino acids and GSH in an essentially aqueous buffer medium at physiological pH. The switch on the luminescence response at 535 nm could be utilized for achieving a lower detection limit of 0.286 μM for cyanide ion and this value was much lower than the threshold cyanide ion concentration of 1.9 μM for safe drinking water set by WHO. Specificity and the visually detectable change in solution luminescence at a $[CN^-]$ of 1.9 μM offers the opportunity to use this reagent as an optical sensor for in-field applications. The release of CN^- and/or HCN (at physiological pH) from amygdalin and mandelonitrile by important enzymes like β-glucosidase and hydroxynitrile lyase, respectively, could also be probed by monitoring the luminescence enhancement of probe **1** and this also helped us in developing an efficient and sensitive assay for two important enzymatic reactions. Importantly, this reagent showed insignificant toxicity towards live MDA-MB-231 cells and the results of the imaging studies further revealed that this chemodosimetric reagent could be utilized for the detection of cyanide ion uptake in live cells. Imaging studies using TIRF microscopy showed that the sole dependence on the increase in the luminescence intensity of the sensor within single cell studies might not provide all the necessary information while exploring the cellular uptake of CN^-. In contrast, spatially-resolved fluorescence spectroscopy measurements performed over a large number of microscopic domains (over several cells) reveal the overall shift in distribution of transition energies as well as integrated emission intensities. This demonstrates that a combination of both spectral shift and emission enhancement provides more conclusive evidence of the cellular uptake of cyanide, and offers a way to probe changes in the sensory response due to variation in local environments within cells and that due to cyanide detection. We are exploring how such spatially-resolved spectral data can be better analyzed to extract more quantitative information on the non-uniformity in the relative proportion of analytes at various local sub-cellular regions.

Acknowledgements

A.D. acknowledges DST (India) Grant (SB/S1/IC-23/2013) and CSIR-NCL for research grant through MLP 028226 for supporting this research. H.A., M.G., and DKS acknowledge CSIR for their research fellowships. AC acknowledges CSIR research grant and IRCC, IIT Bombay, for initial funding. The authors thank Dr Shamik Sen of Bioscience and Bio-Engineering, IIT Bombay, for recording fluorescence images.

Notes and references

1 (*a*) R. Dutzler, E. B. Campbell and R. Mackinnon, *Science*, 2003, **300**, 108–112; (*b*) H. Luecke and F. A. Quiocho, *Nature*, 1990, **347**, 402–406; (*c*) J. W. Pflugrath and F. A. Quiocho, *Nature*, 1985, **314**, 257–260; (*d*) X. Lou, D. Ou, Q. Li and Z. Li, *Chem. Commun.*, 2012, **48**, 8462–8477; (*e*) H. A. Anila, U. G. Reddy, F. Ali, N. Taye, S. Chattopadhyay and A. Das, *Chem. Commun.*, 2015, **51**, 15592–15595; (*f*) F. Ali, H. A. Anila, N. Taye, R. Gonade, S. Chattopadhyay and A. Das, *Chem. Commun.*, DOI: 10.1039/C5CC07450A; (*g*) U. G. Reddy, H. A. Anila, F. Ali, N. Taye, S. Chattopadhyay and A. Das, *Org. Lett.*, DOI: 10.1021/acs.orglett.5b02568.

2 J. Taylor, N. Roney, C. Harper, M. Fransen and S. Swarts, Toxicological Profile for Cyanide, *US Department of Health and Human Services*, Atlanta, GA, 2006, pp. 6–7.

3 (*a*) G. D. Muir, *Hazards in the chemical laboratory*, The Royal society of Chemistry, London, UK, 1977; (*b*) B. Vennesland, E. F. Conn, J. Knownles, J. Westly and F. Wising, *Cyanide in Biology*, Academic London, 1981.

4 S. I. Baskin and T. G. Brewer, in *Medical Aspects of Chemical and Biological Warfare*, ed. F. Sidell, E. T. Takafuji and D. R. Franz, TMM Publications, Washington, DC, 1997, ch. 10, pp. 271–286.

5 R. Takano, *J. Exp. Med.*, 1916, **24**, 207–211.

6 (*a*) D. A. Dzombak, R. S. Ghosh and G. M. Wong-Chong, *Cyanide in Water and Soil: Chemistry, Risk, and Management*, CRC Press, Boca Raton, 2006; (*b*) C. Young, L. Tidwell and C. Anderson, *Cyanide: Social Industrial and Economic Aspects*, TMS (The Minerals, Metals, and Materials Society), Warrendale, 2001.

7 (*a*) *Cyanide in Biology*, ed. L. P. Solomonson, B. Vennesland, E. E. Conn, C. J. Knowles, J. Westley and F. Wissing, Academic Press, London, 1981; (*b*) O. S. A. Oluwole,

A. O. Onabolu, K. Mtunda and N. Mlingi, *J. Food Compos. Anal.*, 2007, **20**, 559–567.

8 (*a*) *Guidelines for Drinking-Water Quality*, ed. M. Sheffer, World Health Organization, Geneva, 1996; (*b*) Y. Kim, H.-S. Huh, H. M. Lee, Y. I. L. Lenov, H. Zhao and F. P. Gabbaï, *Chem. – Eur. J.*, 2011, **17**, 2057–2062; (*c*) Q. Lin, X. Liu, T.-B. Wei and Y.-M. Zhang, *Chem. – Asian J.*, 2013, **8**, 3015–3021.

9 (*a*) Z. Xu, X. Chen, H. N. Kim and J. Yoon, *Chem. Soc. Rev.*, 2010, **39**, 127–137; (*b*) K. Kaur, R. Saini, A. Kumar, V. Luxami, N. Kaur, P. Singh and S. Kumar, *Coord. Chem. Rev.*, 2012, **256**, 1992–2028.

10 (*a*) F. Wang, L. Wang, X. Chen and J. Yoon, *Chem. Soc. Rev.*, 2014, **43**, 4312–4324; (*b*) S. Das, S. Biswas, S. Mukherjee, J. Bandyopadhyay, S. Samanta, I. Bhowmick, D. K. Hazra, A. Ray and P. P. Paruui, *RSC Adv.*, 2014, **4**, 9656–9659; (*c*) C. H. Lee, H. J. Yoon, J. S. Shim and W. D. Jang, *Chem. – Eur. J.*, 2012, **18**, 4513–4516; (*d*) S. Saha, A. Ghosh, P. Mahato, S. Mishra, S. K. Mishra, E. Suresh, S. Das and A. Das, *Org. Lett.*, 2010, **12**, 3406–3409; (*e*) K. Lee, H. Kim, G. Kim, I. Shin and J. Hong, *Org. Lett.*, 2008, **10**, 49–51; (*f*) S. Nam, X. Chen, J. Lim, S. H. Kim, S. Kim, Y. Cho, J. Yoon and S. Park, *PLoS One*, 2011, **6**, e21387.

11 (*a*) A. O. El-Ballouli, Y. Zhang, S. Barlow, S. R. Marder, M. H. Al-Sayah and B. R. Kaafarani, *Tetrahedron Lett.*, 2012, **53**, 661–665; (*b*) N. Gimeno, X. Li, J. R. Durrant and R. Vilar, *Chem. – Eur. J.*, 2008, **14**, 3006–3012; (*c*) X. Lv, J. Liu, Y. Liu, Y. Zhao, M. Chen, P. Wang and W. Guo, *Org. Biomol. Chem.*, 2011, **9**, 4954–4958; (*d*) B. Akhuli, I. Ravikumar and P. Ghosh, *Chem. Sci.*, 2012, **3**, 1522–1530; (*e*) X. Cheng, H. Jia, J. Feng, J. Qin and Z. Li, *J. Mater. Chem. B*, 2013, **1**, 4110–4114.

12 (*a*) V. Bhalla, H. Singh and M. Kumar, *Dalton Trans.*, 2012, **41**, 11413–11418; (*b*) X. Chen, S. W. Nam, G. H. Kim, N. Song, Y. Jeong, I. Shin, S. K. Kim, J. Kim, S. Park and J. Yoon, *Chem. Commun.*, 2010, **46**, 8953–8955; (*c*) Y. Liu, X. Lv, Y. Zhao, J. Liu, Y. Q. Sun, P. Wang and W. Guo, *J. Mater. Chem.*, 2012, **22**, 1747–1750; (*d*) K. P. Divya, S. Sreejith, B. Balakrishna, P. Jayamurthy, P. Anees and A. Ajayaghosh, *Chem. Commun.*, 2010, **46**, 6069–6071; (*e*) H. C. Gee, C. H. Lee, Y. H. Jeong and W. D. Jang, *Chem. Commun.*, 2011, **47**, 11963–11965.

13 (*a*) J. Y. Jo, A. Olasz, C. H. Chen and D. Lee, *J. Am. Chem. Soc.*, 2013, **135**, 3620–3623; (*b*) S. Goswami, A. Manna, S. Paul, A. K. Das, K. Aich and P. K. Nandi, *Chem. Commun.*, 2013, **49**, 2912–2914; (*c*) Y. Hao, W. Chen, L. Wang, B. Zhou, Q. Zang, S. Chena and Y. N. Liu, *Anal. Methods*, 2014, **6**, 2478–2483; (*d*) S. Pramanik, V. Bhalla and M. Kumar, *ACS Appl. Mater. Interfaces*, 2014, **6**, 5930–5939; (*e*) S. Khatua, D. Samanta, J. W. Bats and M. Schmittel, *Inorg. Chem.*, 2012, **51**, 7075–7086; (*f*) X. Lv, J. Liu, L. Liu, Y. Zhao, M. Chen, P. Wang and W. Guo, *Sens. Actuators, B*, 2011, **158**, 405–410.

14 (*a*) J. Liu, Y. Liu, Q. Liu, C. Li, L. Sun and F. Li, *J. Am. Chem. Soc.*, 2011, **133**, 15276–15279; (*b*) X. Cheng, R. Tang, H. Jia, J. Feng, J. Qin and Z. Li, *ACS Appl. Mater. Interfaces*, 2012, **4**, 4387–4392; (*c*) L. Yuan, W. Lin, Y. Yang, J. Song and J. Wang, *Org. Lett.*, 2011, **13**, 3730–3733; (*d*) Y. Zhang, D. Li, Y. Li and J. Yu, *Chem. Sci.*, 2014, **5**, 2710–2716; (*e*) W. C. Lin, S. K. Fang, J. W. Hu, H. Y. Tsai and K. Y. Chen, *Anal. Chem.*, 2014, **86**, 4648–4652.

15 (*a*) M. Sun, S. Wang, Q. Yang, X. Fei, Y. Li and Y. Li, *RSC Adv.*, 2014, **4**, 8295–8299; (*b*) X. Huang, X. Gu, G. Zhang and D. Zhang, *Chem. Commun.*, 2012, **48**, 12195–12197; (*c*) Z. Yang, Z. Liu, Y. Chen, X. Wang, W. He and Y. Lu, *Org. Biomol. Chem.*, 2012, **10**, 5073–5076; (*d*) X. Lv, J. Liu, Y. Liu, Y. Zhao, Y. Q. Sun, P. Wang and W. Guo, *Chem. Commun.*, 2011, **47**, 12843–12845.

16 (*a*) R. Guliyev, S. Ozturk, E. Sahin and E. U. Akkaya, *Org. Lett.*, 2012, **14**, 1528–1531; (*b*) C. R. Wade and F. P. Gabbaï, *Inorg. Chem.*, 2010, **49**, 714–720; (*c*) B. Garg and Y.-C. Ling, *Chem. Commun.*, 2015, **51**, 8809–8812.

17 (*a*) G. U. Reddy, P. Das, S. Saha, M. Baidya, S. K. Ghosh and A. Das, *Chem. Commun.*, 2013, **49**, 255–257; (*b*) D. A. Jose, M. Elstner and A. Schiller, *Chem. – Eur. J.*, 2013, **19**, 14451–14457.

18 (*a*) J. L. Reymond, V. S. Fluxá and N. Maillard, *Chem. Commun.*, 2009, 34–46; (*b*) T. Desmet, W. Soetaert, P. Bojarov, V. Křen, L. Dijkhuizen, V. Eastwick-Field and A. Schiller, *Chem. – Eur. J.*, 2012, **18**, 10786–10801.

19 (*a*) S. Yang, Z. Jiang, Q. Yan and H. Zhu, *J. Agric. Food Chem.*, 2008, **56**, 602–608; (*b*) A. Wallecha and S. Mishra, *Biochim. Biophys. Acta*, 2003, **1649**, 74–84.

20 (*a*) D. R. Haisman and D. J. Knight, *Biochem. J.*, 1967, **103**, 528.

21 (*a*) J. Vetter, *Toxicon*, 2000, **38**, 11–36; (*b*) M. Sharma, N. N. Sharma and T. C. Bhalla, *Enzyme Microb. Technol.*, 2005, **37**, 279–294.

22 S. Madhu, D. K. Sharma, S. K. Basu, S. Jadhav, A. Chowdhury and M. Ravikanth, *Inorg. Chem.*, 2013, **52**, 11136–11145.

23 M. Hu, J. Fan, H. Li, K. Song, S. Wang, G. Cheng and X. Peng, *Org. Biomol. Chem.*, 2011, **9**, 980–983.

24 (*a*) Y. Zhao and Z. Zhong, *Org. Lett.*, 2006, **8**, 4715–4717; (*b*) R. Hu, J. Feng, D. Hu, S. Wang, S. Li, Y. Li and G. Yang, *Angew. Chem.*, 2010, **122**, 5035–5038; (*c*) T. Balos, S. Royo, R. Martìnez- Máñnez, F. Sancenón, J. Soto, A. M. Costero, S. Gil and M. Parra, *New J. Chem.*, 2009, **33**, 1641–1645; (*d*) N. Kumari, S. Jha and S. Bhattacharya, *Chem. – Asian J.*, 2014, **9**, 830–837; (*e*) U. G. Reddy, V. Ramu, S. Roy, N. Taye, S. Chattopadhyay and A. Das, *Chem. Commun.*, 2014, **50**, 14421–14424; (*f*) M. Jamkratoke, V. Ruangpornvisuti, G. Tumcharern, T. Tuntulani and B. Tomapatanaget, *J. Org. Chem.*, 2009, **74**, 3919–3922; (*g*) B. S. Kitawat, M. Singh and R. K. Kale, *ACS Sustainable Chem. Eng.*, 2013, **1**, 1040–1044; (*h*) K. Manabe, S. Iimura, M. X. Sun and S. Kobayashi, *J. Am. Chem. Soc.*, 2002, **124**, 11971–11978; (*i*) L. M. Wang, N. Jiao, J. Qiu, J. J. Yu, J. Q. Liu, F. L. Guo and Y. Liu, *Tetrahedron*, 2010, **66**, 339–343; (*j*) S. Balakumar, P. Thanasekaran, E. Rajkumar, J. K. Adaikalasamy, S. Rajagopal, R. Ramaraj, T. Rajendran, B. Manimaran and K.-L. Lu, *Org. Biomol. Chem.*, 2006, **4**, 352–358; (*k*) T. Nishikata and B. H. Lipshutz, *J. Am. Chem. Soc.*, 2009, **131**, 12103–12105.

25 (*a*) P. Béguin, *Annu. Rev. Microbiol.*, 1990, **44**, 219–248; (*b*) T. Fowler, *Biochemistry and Molecular Biology, ACS Symposium Series*, American Chemical Society, Washington, DC, 1993, vol. 533, pp. 56–65.

26 G. A. Grabowski, A. Berg-Fussman and M. Grace, *Biochemistry and Molecular Biology, ACS Symposium Series*, American Chemical Society, Washington, DC, 1993, vol. 533, pp. 66–82.
27 (*a*) E. E. Conn, Cyanide and cyanogenic glycosides, in *Herbivores, Their Interactions with Secondary Plant Metabolites*, ed. G. A. Rosenthal and D. H. Janzen, Academic Press, New York, 1979, pp. 387–412; (*b*) D. P. Dharmawardhana, B. E. Ellis and J. E. Carlson, *Plant Physiol.*, 1995, **107**, 331–339; (*c*) A. Falk and L. Rask, *Plant Physiol.*, 1995, **108**, 1369–1377.
28 (*a*) B. V. McCleary, D. Mangan, R. Daly, S. Fort, R. Ivory and N. McCormack, *Carbohydr. Res.*, 2014, **385**, 9–17; (*b*) D. Mangan, B. V. McCleary, A. Liadova, R. Ivory and N. McCormack, *Carbohydr. Res.*, 2014, **395**, 47–51.
29 (*a*) T. Yamashita, T. Sano, T. Hashimoto and K. Kanazawa, *Int. J. Food Sci. Technol.*, 2007, **42**, 70–75.
30 (*a*) Y. B. Tewari and R. N. Goldberg, *J. Biol. Chem.*, 1989, **264**, 3966–3971; (*b*) F. F. Zanoelo, M. D. T. D. M. L. Polizeli, H. F. Terenzi and J. A. Jorge, *FEMS Microbiol. Lett.*, 2004, **240**, 137–143.

